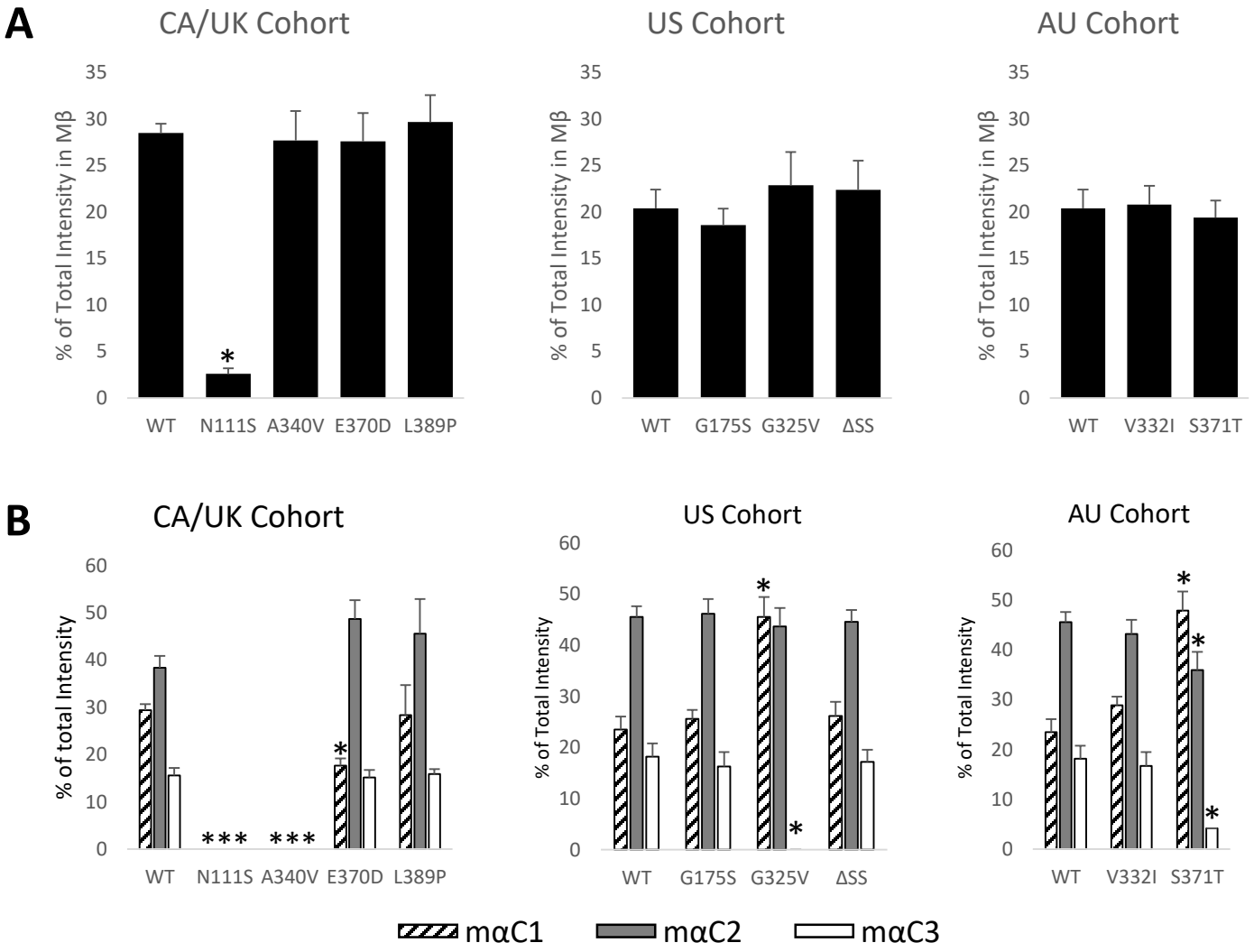

Supplemental Figure 1. Quantification of Western Blots (A) Quantification of the amount of mature Mβ processing form relative to the immature P1 form in the western blots from Figure 2. Relative amounts were quantified for three biological replicates using ImageJ. Significantly different (student's 2-tailed T-test [$p<0.05$]) relative amount of Mβ was detected only for p.N111S which showed a significant processing deficit. **(B)** Quantification of the relative amounts of mαC1 (hatched bar), mαC2 (solid grey bar), or mαC3 (white bar) relative to the immature mα form in the western blots from Figure 2C. Relative amounts were quantified for three biological replicates using ImageJ. Significantly different (student's 2-tailed T-test [$p<0.05$]) relative amounts of mαC1, mαC2, or mαC3 were detected for p.E370D, p.G325V, p.S371T.

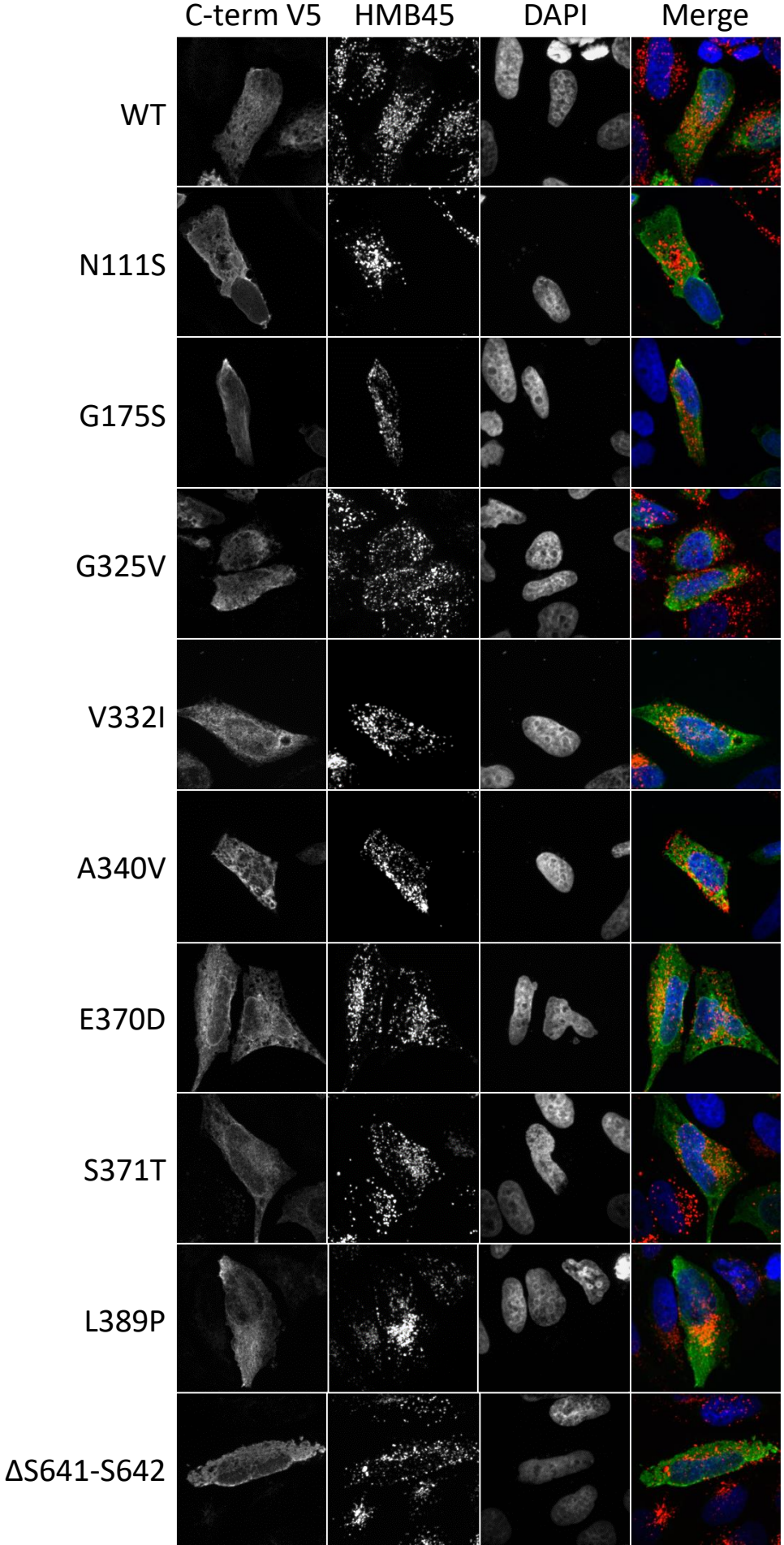
C-term V5
HMB45
DAPI
Merge
WT
N111S
G175S
G325V
V332I
A340V
E370D
S371T
L389P
ΔS641-S642

Supplemental Figure 2. Immunofluorescence microscopy shows that PMEL variants appear to traffic normally (A) V5-tagged PMEL (green) appears mesh like suggesting ER localization in all variants. No differences between PMEL-WT and any PDS/PG associated variants were observed. HMB45-reactive PMEL (red) appears correctly as cytoplasmic puncta suggesting correct trafficking to a subset of endosomes and no clear retention in the Golgi. The same pattern was observed for all variants suggesting no defects in trafficking. DAPI staining was used to show the nucleus (blue).

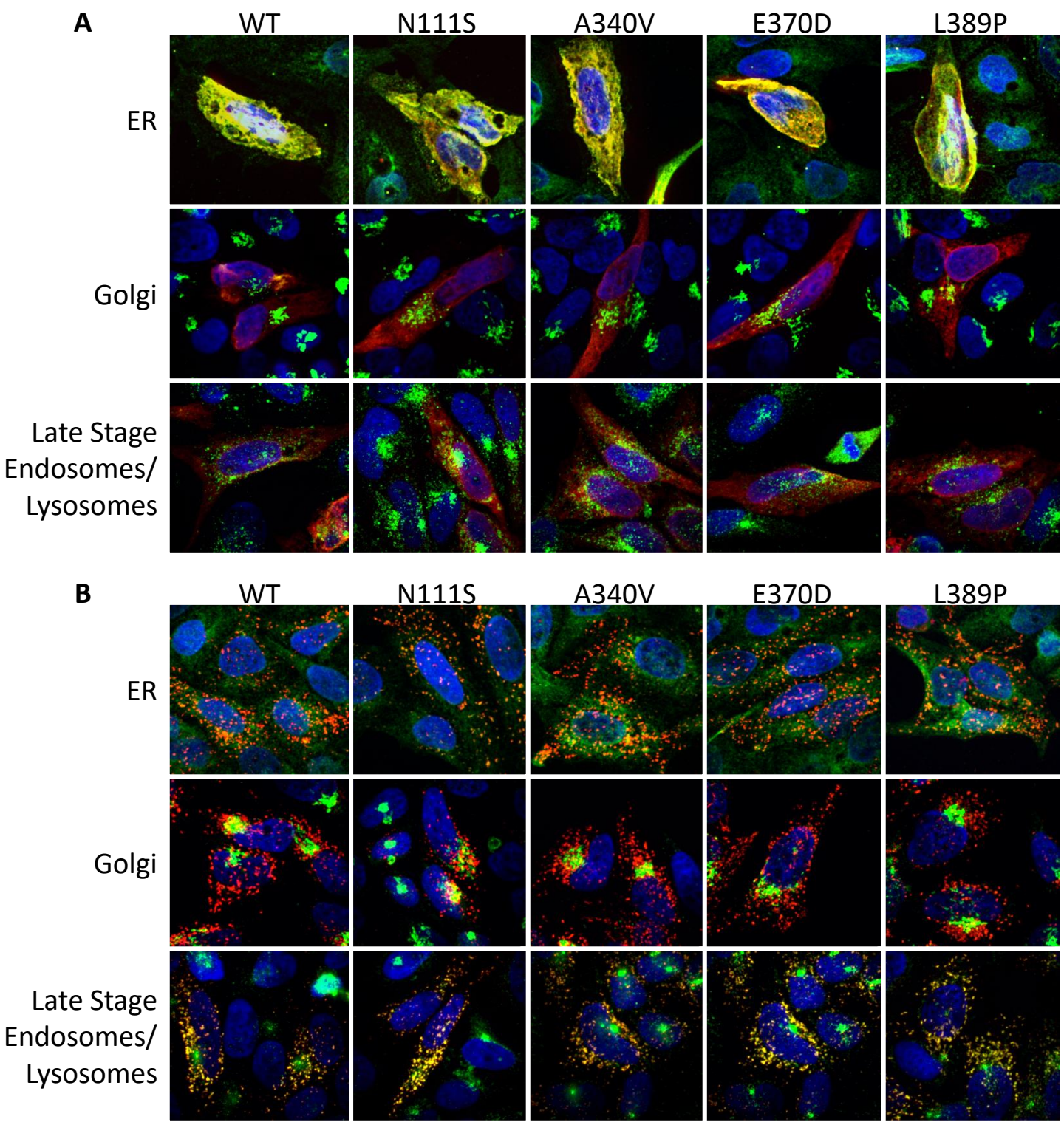

Supplemental Figure 3. Subcellular colocalization immunofluorescence demonstrates that PMEL variants do not impair trafficking To confirm that variants do not impair trafficking, a more thorough subcellular colocalization analysis for a subset of variants was undertaken. **(A)** V5-tagged PMEL (red) colocalizes with ER (green, upper panels) and partially with Golgi (green, middle panels), but not endosomal markers (green, bottom panels). No differences between WT PMEL and PDS/PG associated PMEL variants were detected. **(B)** HMB45-reactive mature sialylated PMEL (red) shows correct trafficking to a subset of endosomes (green, bottom panels), and is not retained within the ER (green, top panels) or Golgi (green, middle panels).

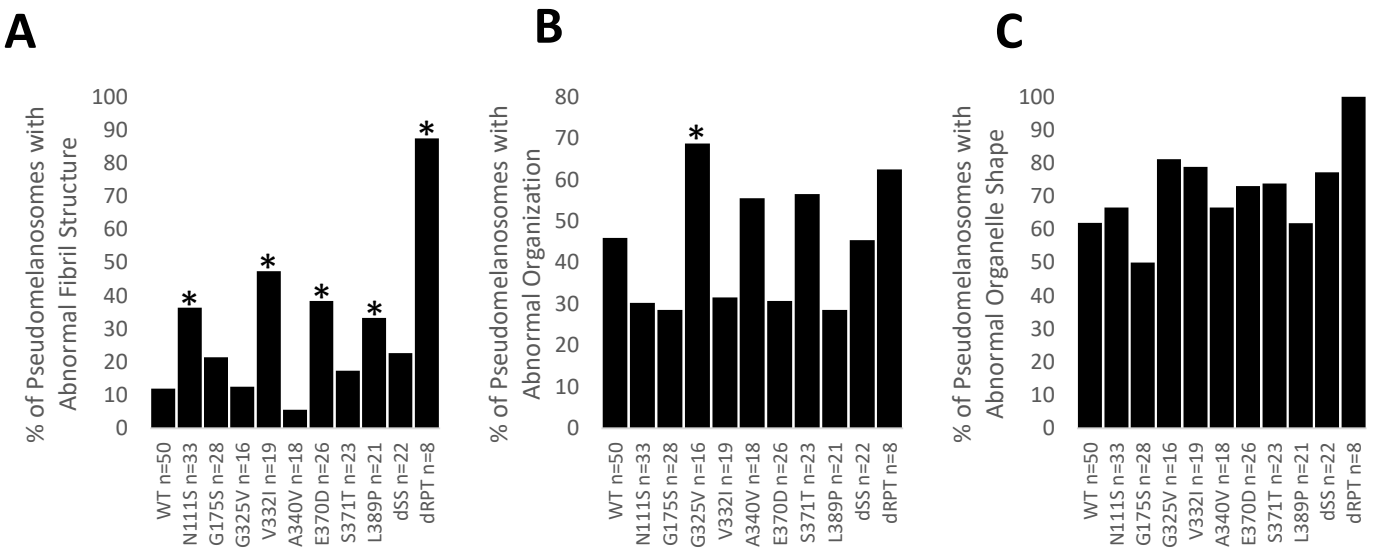

Supplemental Figure 4. Quantification of ultrastructural defects observed in pseudomelanosomes show four variants with abnormal fibril formation and one variant with abnormal organization. Pseudomelanosomes were scored for three features (n=# of pseudomelanosomes scored). Proportion of pseudomelanosomes exhibiting a certain defect were compared using a one-tailed Z-statistic proportion test ($p<0.05$). **(A)** Pseudomelanosomes were scored for the appearance of abnormal fibrils. PMEL-N111S, -V332I, -E370D, and -L389P contained significantly more pseudomelanosomes with abnormal fibrils ($p<0.05$). **(B)** Pseudomelanosomes were scored for abnormal fibril organization. Significantly more pseudomelanosomes with abnormal fibril organization were observed for PMEL-G325V than WT ($p<0.05$). (C)) Pseudomelanosomes were scored for abnormal organelle shape. No significant difference in the proportion of abnormally shaped pseudomelanosomes between PMEL-WT and PDS/PG associated variants was observed.

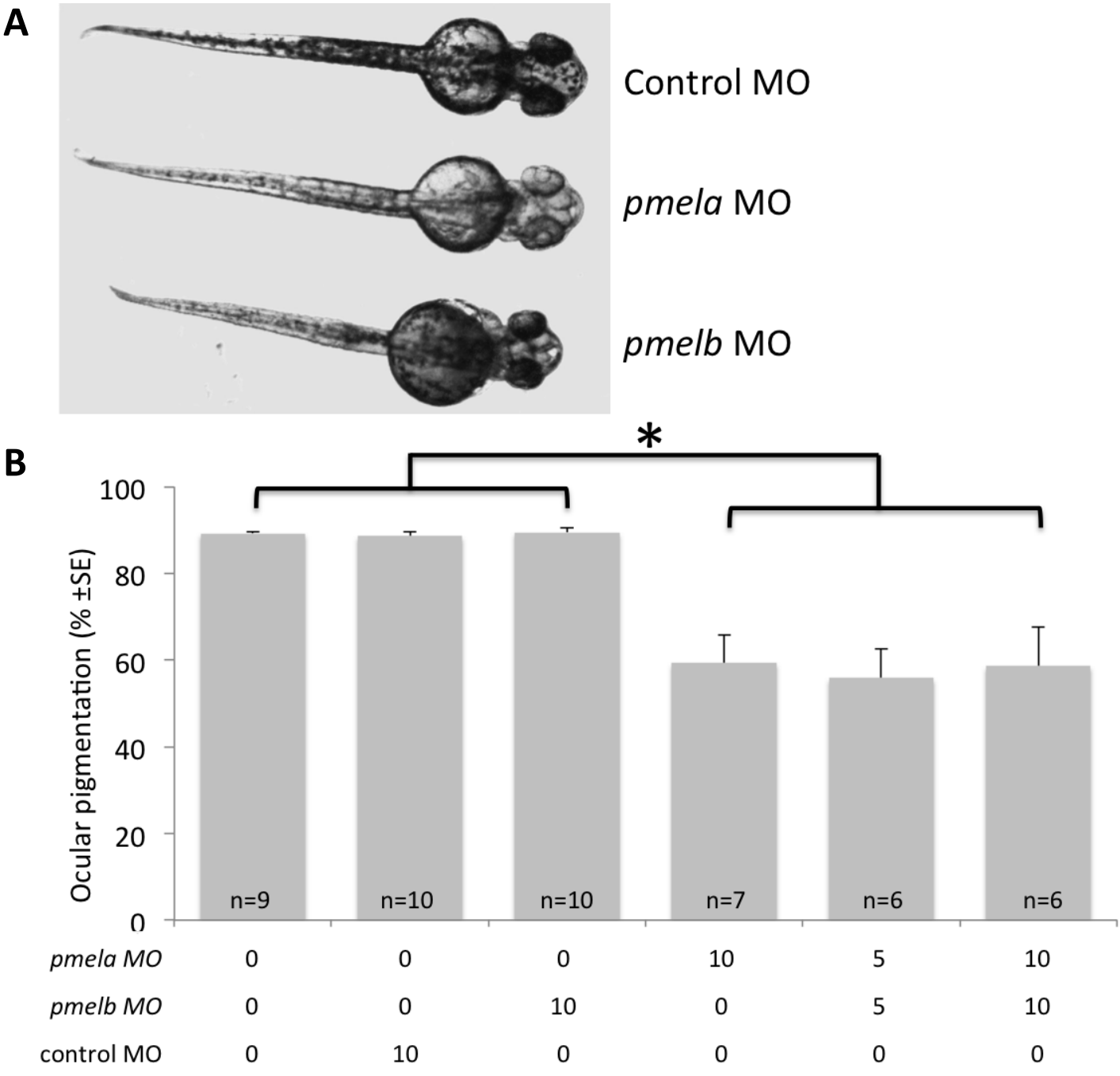

Supplemental Figure 5. Disrupting homolog of *PMEL* in zebrafish demonstrates its requirement for normal pigmentation *in vivo*. **A**. Representative images of zebrafish larvae (dorsal view) showing pigmentation levels following morpholino knockdown of *pmela* or *pmelb*. **B**. Quantification of eye pigmentation from dorsal view of zebrafish at 3 days post-fertilization, wherein percent of pixels that are pigmented were quantified. Abscissa reports the morpholino injected and dose in ng per larva. * indicates all three bars on left are significantly different than all three bars on right at $p<0.05$ by ANOVA; sample sizes (n) are number of larvae examined. Similar results were found when whole body pigmentation and/or when 2 days post-fertilization larvae were quantified.

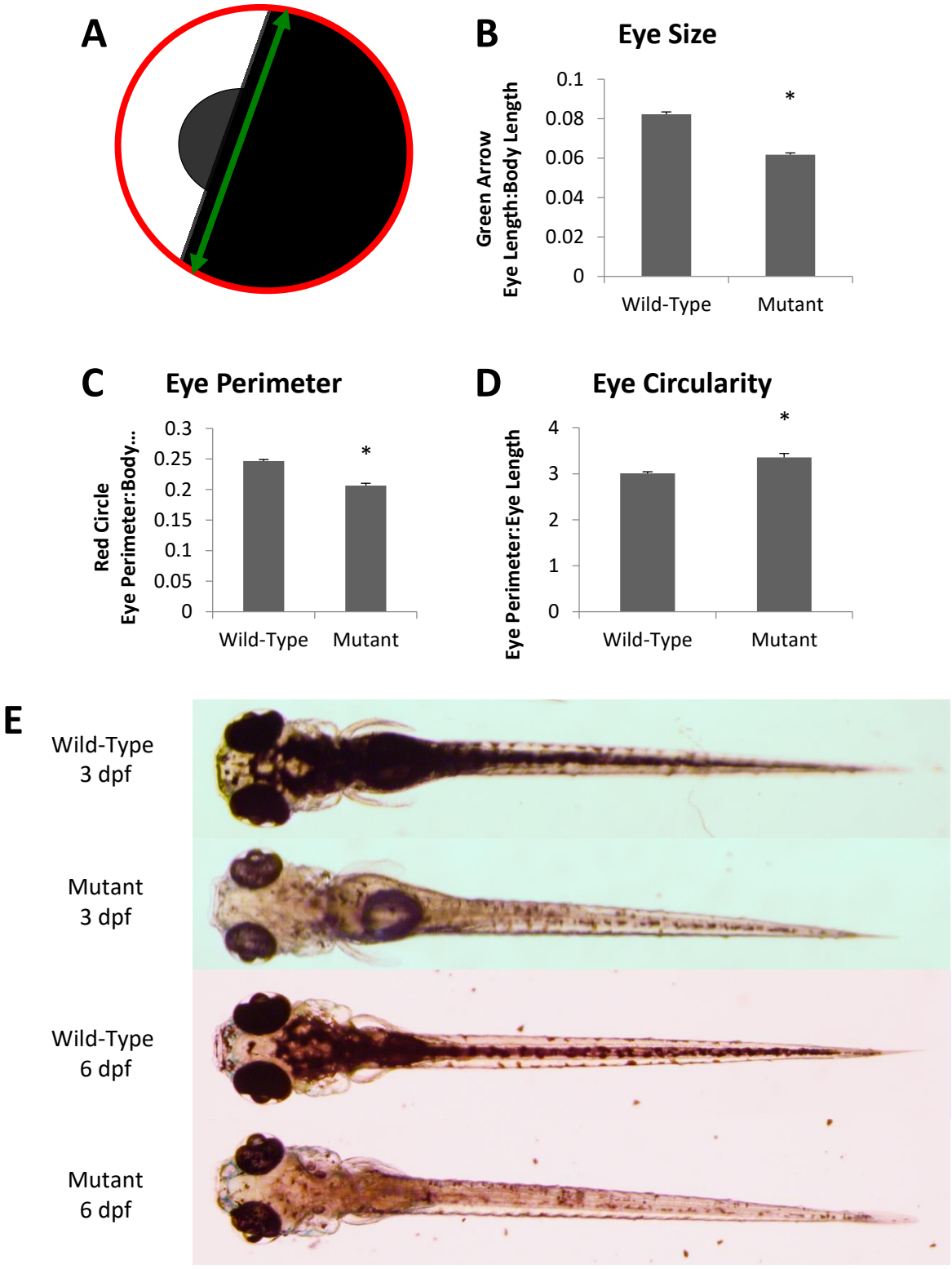

Supplemental Figure 6. (A) Schematic of the measurements that were taken of the larval zebrafish eyes where yellow-eye length and red-eye perimeter. (**B)** Quantification of the eye length to body length ratio in zebrafish larvae. **(C)** Quantification of the eye perimeter to body length ratio in zebrafish larvae. (**D)** Quantification of the perimeter to eye length ratio in zebrafish larvae. Sample sizes: pigmented (n=14), abnormally pigmented (n=3). P-value < 0.005 using one tailed t-tests. (**E)** Larval zebrafish at 3 dpf and 6 dpf without and with the 11-base pair homozygous deletion.

Supplemental Table 1. Family 2 - Filtered Whole Exome Sequencing Variants

Gene	HGVS cDNA	HGVS Protein	dbSNP ID	gnomAD Allele Freq.	Gene Ontology - Biological Process
ANKHD1	NM_017747.2: c.3980C>T	NP_060217.1: p.Thr1327Met	n/a	0.00001219	innate immune response
ARHGEF40	NM_018071.4: c.937G>A	NP_060541.3: p.Gly313Arg	rs374664276	0.0001215	regulation of Rho protein signal transduction
GSTA5	NM_153699.1: c.282G>A	NP_714543.1: p.Met94Ile	rs775966246	0.00001834	glutathione metabolic process
HCK	NM_002110.3: c.1049delG	NP_002101.2: p.Gly350AlafsTer98	n/a	n/a	cell adhesion; cell differentiation; cytokine-mediated signaling pathway; Fc-gamma receptor signaling pathway involved in phagocytosis; inflammatory response; innate immune response-activating signal transduction; integrin-mediated signaling pathway; interferon-gamma-mediated signaling pathway; leukocyte degranulation; leukocyte migration involved in immune response; lipopolysaccharide-mediated signaling pathway; mesoderm development; negative regulation of apoptotic process; peptidyl-tyrosine autophosphorylation; peptidyl-tyrosine phosphorylation; positive regulation of actin cytoskeleton reorganization; positive regulation of actin filament polymerization; positive regulation of cell proliferation; protein autophosphorylation; protein phosphorylation; regulation of cell shape; regulation of defense response to virus by virus; regulation of inflammatory response; regulation of phagocytosis; regulation of podosome assembly; regulation of sequence-specific DNA binding transcription factor activity; respiratory burst after phagocytosis; transmembrane receptor protein tyrosine kinase signaling pathway; viral process
KCNH6	NM_030779.3: c.263G>T	NP_110406.1: p.Gly88Val	n/a	n/a	regulation of membrane potential
OR4M1	NM_001005500.1: c.300G>C	NP_001005500.1: p.Gln100His	n/a	0.000004061	detection of chemical stimulus involved in sensory perception; G-protein coupled receptor signaling pathway
PMEL	NM_001200054.1: c.1019C>T	NP_001186983.1: p.Ala340Val	rs756974126	0.00005796	developmental pigmentation; melanin biosynthetic process; melanosome organization
POLR3E	NM_001258033.1: c.200C>G	NP_001244962.1: p.Pro67Arg	rs368180184	0.000004063	defense response to virus; innate immune response; positive regulation of type I interferon production; transcription from RNA polymerase III promoter
SLITRK5	NM_015567.1: c.1616A>G	NP_056382.1: p.His539Arg	n/a	n/a	adult behavior; axonogenesis; cardiovascular system development; chemical synaptic transmission; dendrite morphogenesis; grooming behavior; positive regulation of synapse assembly; response to xenobiotic stimulus; skin development; striatum development
SNPH	NM_014723.3: c.803T>C	NP_055538.2: p.Val268Ala	n/a	n/a	brain development; neuron differentiation; neurotransmitter secretion; synaptic vesicle docking
TESK2	NM_007170.2: c.1475G>A	NP_009101.2: p.Arg492Lys	rs373927435	0.00004072	actin cytoskeleton organization; focal adhesion assembly; intracellular signal transduction; protein phosphorylation;

The cDNA and protein notations shown conform to the Human Genome Variation Society (HGVS) recommendations.

Supplemental Table 2. Primer Sequences for Targeted Resequencing of *PMEL*

Targeted Region	Primer 1 Sequence (5'→ 3')	Primer 2 Sequence (5'→ 3')
PMEL_ex1	TCGCTCTTGTCAATTTGGCC	GACAGTGTCGGGGTATGCTA
PMEL_ex2	GCAGGATGGGAAAGCAATGT	CGCCTGAAATATTGCCGCTA
PMEL_ex3	TGCACTTCGAATGTGAGAATGA	TCCAGGGAAGTTCAAGGCAA
PMEL_ex4	GTGGGAGTGGGATGAGGAAA	AAGTAGAGAAGGAAGGGGCA
PMEL_ex5	TCTCTGATACCCTGGGAGCA	TGAGGAAGAGTTGCCAGAAAG
PMEL_ex6	CCCCATATCACAGCCTTCCA	TTTCCAGTCCATCCAAGCCT
PMEL_ex7.1	GAGGGTGTGGCTGTGAAAG	ATGTGGTTCCAGAGGGCTC
PMEL_ex7.2	AGTTCCAGGCACCACAGATG	GAACCTCATTCGCACTGATACT
PMEL_ex8	ATTCCAAGCCTGTGACTCCA	ATCCCATCCCTGTGCTTTCA
PMEL_ex9,10	GAGGCCAGGTAGAGGAATCC	CAGGCATGATAAGCTGGGTG
PMEL_ex10,11	CCTCAATGTGTCTCTGGCTG	CCCAGGTCCTACAAGCAAGA
PMEL_ex12	AGGGGAGGAAGCTAGGATCA	TGGGATCTGCTAAGTAAGTGGT

The Illumina Nextera Transposase Adaptor sequences (5'-TCGTCGGCAGCGTCAGATGTGTATAAGAGACAG-3' and 5'-GTCTCGTGGGCTCGGAGATGTGTATAAGAGACAG-3') were respectively added to the 5' ends of all Primer 1 and Primer 2 sequences.

Supplemental Table 3. Morpholinos (MOs) used to disrupt zebrafish homologues of PMEL

MO Name	Dose	Sequence (5'→ 3')	ZFin.org ID	Reference
pmela	10 ng	GATGAGAGATGTCCACATGATGACC	ZDB-MRPHLNO-150618-3	1
pmelb	10 ng	AGGAAACAGTGTTTACTTACTTGTT	n/a	Current work

Supplemental Table 4. Zebrafish primers

Sequence Description	Oligonucleotide Sequence
CRISPR Binding Sequence	5’-GATAACGTGCAAATCGAGTT-3’
SP6 Promoter	5’-ATTTAGGTGACACTATA-3’
gRNA Backbone	5’-GTTTTAGAGCTAGAAATAGCAAG-3’
Constant Oligomer	5’-AAAAGCACCGACTCGGTGCCACTTTTTCAAGTTGATAACGGACTAGCC TTATTTTAACTTGCTATTTCTAGCTCTAAAAC-3’
PCR Forward Primer	5’-CAGGCGGTTTAAGGAGTACCA-3’
PCR Reverse Primer	5’-GTGACTGTAGACCAAATAAAGCAG-3’
qPCR Forward Primer	5’-GCGACACTCGGAGTTCTGTT-3’
qPCR Reverse Primer	5’-TCACACCACGCGTCCCAGCA-3’

Supplemental Table 5. Non-synonymous PMEL Variants in Controls

Protein NP_001186983.1	Mutation	cDNA NM_001200054.1	dbSNP ID	Allele Frequency gnomAD MAF§	Allele Frequency Current Study (# alleles / 1799)	PMEL Domain*
p.Leu12Val	L12V	c.34T>G	n/a	n/a	0.0011 (2)	Sig
p.Gln30Glu	Q30E	c.88C>G	n/a	n/a	0.0011 (2)	NTF
p.Val213Ala	V213A	c.638T>C	n/a	n/a	0.0011 (2)	CAF
p.Ile270Leu	I270L	c.808A>C	rs142781578	n/a	0.0006 (1)	PKD
p.Pro320Thr	P320T	c.958C>A	n/a	n/a	0.0022 (4)	RPT
p.Ser350Phe	S350F	c.1049C>T	rs765152357	0.00005426	0.0006 (1)	RPT
p.Pro354Ser	P354S	c.1060C>T	n/a	n/a	0.0006 (1)	RPT
p.Ala362Val	A362V	c.1085C>T	rs1804189	0.00003097	0.0011 (2)	RPT
p.Pro363Ser	P363S	c.1087C>T	rs61752491	0.00009290	0.0094 (17)	RPT
p.Glu370Asp	E370D	c.1110G>C	rs17118154	0.00247690	0.0100 (18)	RPT
p.Leu389Pro	L389P	c.1166T>C	rs142410496	0.00075229	0.0006 (1)	RPT
p.Thr447Met	T447M	c.1340C>T	rs113995172	0.00010265	0.0033 (6)	(gap)
p.Gly505Ser	G505S	c.1513G>A	rs76045902	0.00020906	0.0094 (17)	(gap)
p.Gln556Pro	Q556P	c.1667A>C	rs772472625	0.00005289	0.0006 (1)	Kringle
p.Ser562Leu	S562L	c.1685C>T	rs148206928	0.00002326	0.0006 (1)	Kringle
p.Val603Ala	V603A	c.1808T>C	rs57990974	0.00020126	0.0094 (17)	TM

Non-synonymous PMEL variants identified during exome analysis of 1799 ophthalmologically-examined controls. The cDNA and protein notations shown conform to the Human Genome Variation Society (HGVS) recommendations. gnomAD, Genome Aggregation Database; MAF, minor allele frequency; PDS, pigmentary dispersion syndrome; PG, pigmentary glaucoma. §European (Non-Finnish) MAF. *See Figure 2 for PMEL protein domain structure and abbreviations.